Electrostatic charging and charge transport by hydrated amorphous silica under a high voltage direct current electrical field

Carlos Eduardo Perles and Pedro Luiz Onófrio Volpe

Citation: The Journal of Chemical Physics **134**, 214703 (2011); doi: 10.1063/1.3597777

View online: http://dx.doi.org/10.1063/1.3597777

View Table of Contents: http://scitation.aip.org/content/aip/journal/jcp/134/21?ver=pdfcov

Published by the AIP Publishing

Electrostatic charging and charge transport by hydrated amorphous silica under a high voltage direct current electrical field

Carlos Eduardo Perles[a] and Pedro Luiz Onófrio Volpe
Institute of Chemistry, Universidade Estadual de Campinas – UNICAMP, Cidade Universitária Zeferino Vaz, S/N, POB 6154, CEP:13083-970, Campinas, São Paulo, Brazil

(Received 22 February 2011; accepted 15 May 2011; published online 6 June 2011)

This work was initially based on the casual observation of an electrostatic phenomenon, in which particles of amorphous silica were attracted by a dc electrical field. The first observations were recently shown in a communication in this journal. To explain the electrical charge transport process observed in this work, all forces acting on silica particles were estimated and the significant ones were used to formulate a model made up of three elementary steps. Analyzing the experimental observations using this model, it was possible to suggest that electrons can be introduced into and removed from electronic bands of water. © *2011 American Institute of Physics*. [doi:10.1063/1.3597777]

I. INTRODUCTION

Porous materials with high superficial areas, such as silica gel, are recognized for their adsorption and catalytic properties.[1]

Silica is a polymer of silicon oxide composed of tetrahedrons of SiO_4 covalently bonded through the oxygen atoms. It can be described as a cluster of elementary particles that are produced in the first step of a sol-gel process. The clustering process occurs in the second step of the sol-gel process in which the elementary particles join together, producing larger aggregated particles, while the pores are formed by interstitial spaces between these elementary particles in the aggregation.[1,2]

The types and density of silanol groups distributed on the surface define the adsorptive properties of silica. The silanol/siloxane ratio and the silanol type (vicinal, isolated, or geminal) define the chemical properties of the surface and, consequently, the energy and the orientation of the bonds with the adsorbate. Vicinal and geminal silanols can interact simultaneously with some adsorbates as, for instance, water.[1,3]

A very important property of silica is its high adsorption capacity caused by the excess of surface energy due to the discontinuity of the three-dimensional network of the SiO_4. Adsorption is a physical-chemical process that reduces the free energy of the surface through chemical bonds and/or interactions with the adsorbate molecules. In the vapor phase, water molecules adsorb on the silica surface, anchored, mainly, by hydrogen bonds.[1–4]

When the molecules of water in the vapor phase interact with silanol groups on the silica surface, a degree of freedom is lost and the entropy is decreased. The silica surface can impose a spatial organization of, at least, three water layers. In the field force action of the surface forces, this region is known as the *high viscosity boundary layer* (HVBL) and the mobility of water is decreased and the properties are drastically modified. This effect of the surface forces on the structure of the adsorbed water can be observed by the existence of an unfrozen layer even at temperatures as low as 173 K. Studies by differential scanning calorimetry, differential thermal analysis, and inelastic neutron scattering indicate that restrictions on the mobility imposed by the surface forces hinder the molecules closer to the surface from acquiring a crystalline structure (ice I_h or I_c).[3,5–9] Although the organizational degree acquired by these molecules on silica has been extensively studied by several experimental and theoretical techniques, there is still no final definition about this.[9–12]

Using simulations, Yang *et al.* (2004)[13] suggested a structure similar to water filaments, as a unidimensional polymeric chain, with water covering half of a statistical monolayer. He also showed that with monolayer coverage occurs the formation of a structure similar to "ice tesselation," composed of square rings bound together and adhering to the surface of the sílica by hydrogen bonds.

Condensed bulk water presents a structure with a high organizational degree for a liquid, being recognized as a *pseudocrystal* with an electronic structure similar to insulating materials, according to the *Bloch model*.[14] Extended-state bands in condensed water are obtained from the combination of the molecular orbitals $1b^2$ and $3a^1$, electron donors, and $4a^1$ and $2b^2$, electron acceptors,[15–17] and their relative structure can be changed with the geometry and the force of the chemical bonds and the water cluster size, as shown in the simulations by Chipman,[18,19] Lee *et al.*,[20] and Couto *et al.*[21] These papers show how the electronic structure of condensed water is directly influenced by the geometry and size of the water clusters.

Alterations of relative and absolute energy of the water bands can affect properties, such as electrical charging, and allow exploration of the effect of the structural changes imposed by the surface on its electronic properties.

Contact electrical charging is a well-known phenomenon but its mechanism is still not well understood. However, two models have been developed which can, partially, explain the experimental observations: (a) electronic and (b) ionic partitioning.[22,23]

[a]Electronic mail: ceperles@gmail.com. Tel.: +55 19 3521-3429. Fax: +55 19 3521-3023.

The more accepted mechanism is the *electronic* one, in which electrons are transferred from material with higher to that of lower *Fermi level* (energy of the outermost electrons), when they are put into physical contact. The *Fermi level* of metallic electrodes can be modified by temperature and/or a voltage source. Electron transfer can occur in both directions, depending only on the relationship between the *Fermi energy* of the electrode and the conduction band of the insulator or semiconductor in contact with this electrode. The electrons can be added to bulk water or to clusters, generating species such as $(H_2O)^-_n$, known as hydrated electrons, i.e., one electron surrounded by a continuum of water molecules.[24–27] This electron can be localized in a cavity (*s* or *p* type), stabilized by water dipoles or can be in a *quasifree* state, delocalized on several molecules. However, the nature of this electron is still not well known. More information about hydrated electrons can be found in several references.[28–32]

In the case of *ionic partitioning*, ions adhered onto surface are transferred between two surfaces by contact or collision, leaving the surfaces with unbalanced charges when they are separated. These ions can be the counter ions of an ionic solid or can be produced at the contact surfaces by redox reactions.

Both these models are used to explain experimental observations in electrostatic studies but the most suitable seems to depend on the characteristics of the experiment, as shown in recent papers.[24–27] Gouveia and Galembeck[24] showed that water is a source and a sink of electrical charges and, therefore, the increase of the negative potential on the silica surface while water desorption proceeds occurs due to the mechanism of ionic partitioning. Ovchinnikova and Pollack[25] suggested the possibility of electrons being trapped in a network similar to the n and p semiconductor regions.

In this work, we have studied the effect of the surface on the spatial structure of surface water using electrons added and removed from the electronic bands of adsorbed water as electronic probes. In this study, electrical charges were injected into the surface layer under a dc electrical field (EF) up to 375 $V\,mm^{-1}$. A first qualitative analysis of this phenomenon, first described in a recent communication in this journal,[32] will be shown.

II. EXPERIMENTAL SECTION

A. Assembly of the experimental apparatus

The high voltage cylindrical cell (d_{in} = 90 mm, d_{out} = 110 mm, h = 80 mm) was made from PVC with a removable top also of PVC having inner threads for fixation to the cell body with an o-ring at the upper side of the cell body for sealing. At the bottom, a hemispherical glass plate (2 mm thickness) was fixed to the cell body by a PVC ring with inner thread, allowing its exchange if necessary.

The high voltage electrode (aluminum disc d = 10 cm) was fixed inside the cover and the hemispheric glass plate at the bottom of the cell was placed on the grounding electrode (aluminum disc d = 10 cm). These electrodes were assembled to generate an electrical field perpendicular to the electrodes and parallel to the center axis of the cylindrical cell. The electrical field was generated by a dc high voltage source (30 kV, 0.3 mA; Isbiotech). The rate of charge transport was measured as electrical current, on the order of 100 nA, that was amplified (amplifier built in the laboratory) and the signal was converted by an analog/digital acquisition device (USB – 6009, National Instruments). Figure 1 shows a schematic representation of the assembled apparatus.

Light-scattering was used to monitor variations in the number of particles flowing between the two electrodes, i.e, the density of particles flowing between electrodes. The photodetector was assembled on a printed circuit board using an OPT-101 photosensor[33] together with a signal amplification circuit for sensitivity adjustment. A solid-state laser (5 mW) emitting in the red spectral range, aligned with the photodetector window and positioned 90° was used as light source.

The high voltage system (cell + electrodes) was isolated in an acrylic box with lateral holes to permit a dry airflow to the cell, inside of the box. The relative humidity inside of the isolation box (RH_{box}) was maintained below 25% by recirculation of the air through of a drying column containing silica gel with humidity indicator (Merck).

Control of the high voltage source, solenoid valve, *peltier* element (temperature control of dry air for dehydration), and the acquisition of all data (electrical current, dry air temperature, intensity of light-scattering) was done with software developed in LABVIEW®.

B. Pretreatment of the silica gel samples

Three samples of silica gel (Sigma-Aldrich), with different surface properties, were used as shown in Table I. The samples were sieved and dried at 423 K for 24 h. After drying, the samples were placed in a dessicator and maintained under vacuum. The density of surface silanol groups was obtained by thermogravimetry (TGA).[34]

C. Hydration of the silica gel

In the experiments with hydrated silica, the samples, after pretreatment, were put in a chamber with constant relative humidity and temperature (74% ± 1%; T = 298 ± 1 K) (Ref. 36) for a defined period of time (depending on the experiment). The relative humidity inside of this chamber was maintained constant by using a saturated NaCl solution and was monitored by a thermohygrometer (TFA, Maxim II).

D. Experimental procedure of dehydration of the silica exposed to an electrical field

After pretreatment, the dried silica samples were quickly weighed (1.0000 g) and transferred to the humidity chamber for 72 h (adsorption equilibrium). Afterwards, the samples were removed from the humidity chamber, weighed, and quickly transferred to the cell, which was closed and put inside the isolation box. The aluminum electrode, fitted in the inner side of the cover, was immediately connected to the positive pole of the high-voltage source.

Before starting the experiment, the relative humidity inside the isolation box (RH_{box}) was reduced to <25% by recirculation of the box air through the drying column and,

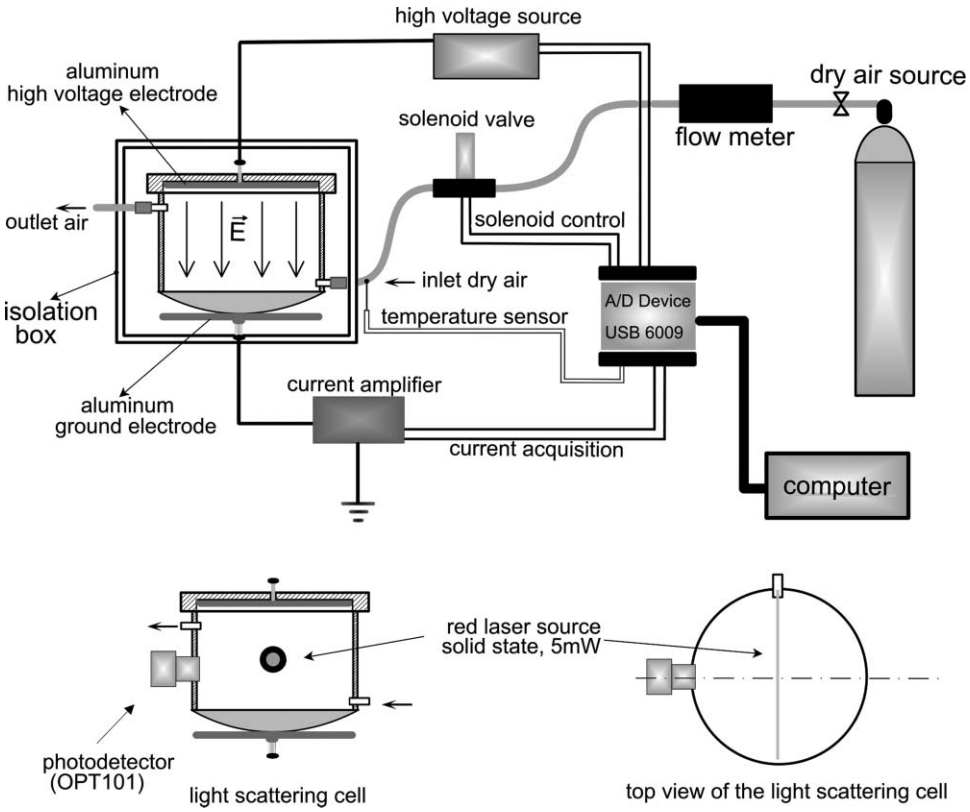

FIG. 1. Upper: Schematic representation of the system assembled for studies in an electrical field. Lower: a representation of the light-scattering cell.

afterwards, the experiment was started by the software, switching on the solenoid valve (opening dry air flow) and the high voltage source.

The slow dehydration of silica gel inside was made by pulling the water vapor of the atmosphere from inside of the cell using a flow of 1 L min^{-1} of dry air.

The gravimetric experiments followed the same procedure above but the whole cell was frequently weighed on a semi-analytical balance, throughout the dehydration time. The curves of electrical current or mass loss vs. dehydration time, (i x t) and ($m H_2O$ x t), respectively, are shown in the same plot.

III. RESULTS

At the beginning it was observed that when a silica sample, initially deposited on hemispherical plate on the lower electrode, was exposed to a dc electrical field of 375 V m^{-1}, the particles were hurled by this electrical field to the high voltage electrode, colliding with it and then returning to the plate on the lower electrode (ground), restarting the cycle. This phenomenon attracted our attention because silica gel is an insulating material in these conditions.

In the next step, after heating the samples of silica gel at T = 423 K for 24 h to dehydrate them, no visible movement of particles in the electrical field was observed. It was possible to conclude that the particle charging could be attributed to the layer of water adsorbed on the silica that, in some way, was electrically charged until the electrostatic force overcame the opposite forces and, consequently, could be attracted to the upper electrode.

Based on these preliminary observations a very interesting study on the capacity of condensed water to store electrical charges in its electronic structure and the possibility to study this electronic structure using injected electrons as probes was developed.

A. Experiments of current vs. intensity of the electrical field

In the first place it was necessary to verify the relationship between the electrical current, variations in the number of flowing particles, and the intensity of the EF.

TABLE I. Surface properties of the silica gel samples obtained by nitrogen adsorption curves using BET (Brunauer, Emmett and Teller) theory and TGA.

Sample	X_m/μm (mean particle size)	Bulk density (d_B/g cm^{-3})[a]	Surface area (A/m^2 g^{-1})	Pore diameter (ϕ_{pore} /nm)	Pore volume (V_p/cm^3 g^{-1})	Silanol groups density (δ_{SiOH} /SiOH nm^{-2})
SG1	172	0.63	616	3.7	0.76	3.3
SG2	170	0.54	537	5.8	0.79	3.8
SG3	173	0.45	319	9.6	0.96	4.8

[a]Values obtained by interpolation with data shown in Ref. 35.

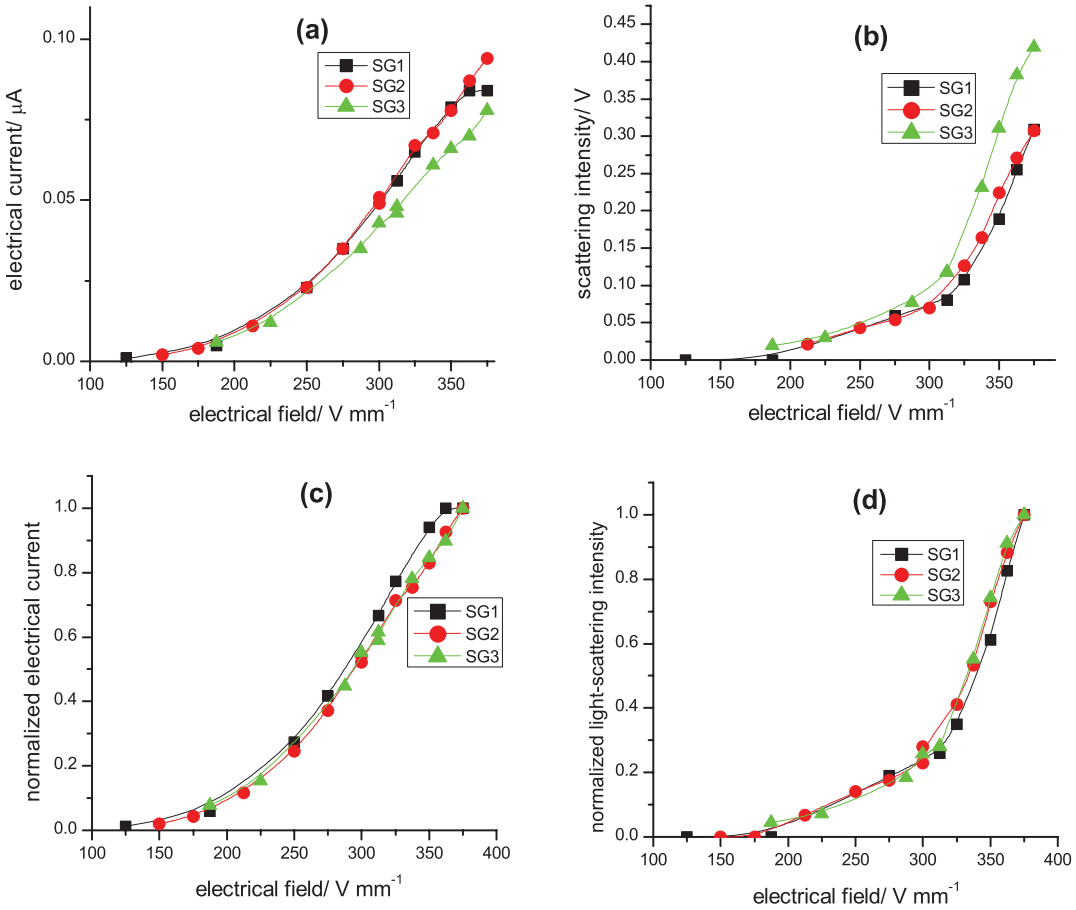

FIG. 2. Curves as functions of the intensity of electrical field: (a) current x EF; (b) light-scattering x EF; (c) normalized current x EF; (d) normalized light-scattering intensity x EF.

When hydrated silica samples are exposed in an increasing electrical field (see Sec. II), the number of flowing particles between the electrodes increases as the electrical current increases, as is shown in Figs. 2(a) and 2(b). In these experiments, the cell was sealed to maintain the humidity constant on the silica surface.

Normalizing the curves in Figs. 2(a) and 2(b) by maximum electrical current, as shown in Figs. 2(c) and 2(d), the same behavior is observed, independent of the surface properties. Analyzing these curves, an electrostatic threshold ($\sim$175 V mm^{-1}) can be noted before a significant amount of particles start to flow. At this point, it can be considered that the electrostatic force ($\vec{F}_E$) annuls the opposing forces ($\vec{F}_{op}$) acting on these particles. In these experiments it was observed that variations in the number of flowing particles and the electrical current transported by these particles are not linear, as can be seen in Fig. 3.

There are two hypotheses to explain this: (1) the density of electrical charges on the particles increases up to 310 V mm^{-1} or (2) when the intensity of the electrical field is increased, heavier particles acquire sufficient electrical charge to annul $\vec{F}_{op}$, transporting more electrical charges by each particle.

Unfortunately, it is not possible to calculate a numerical value of the density of the electrical charges on one particle, because the detection system of the scattered light gives a signal, in volts, proportional to the number of particles flowing but not an absolute number of these flowing particles.

Figures 2(a) and 2(b) also show that in both the light-scattering and the charge transport plots, each sample has different intensities of response, which seem to be related to the

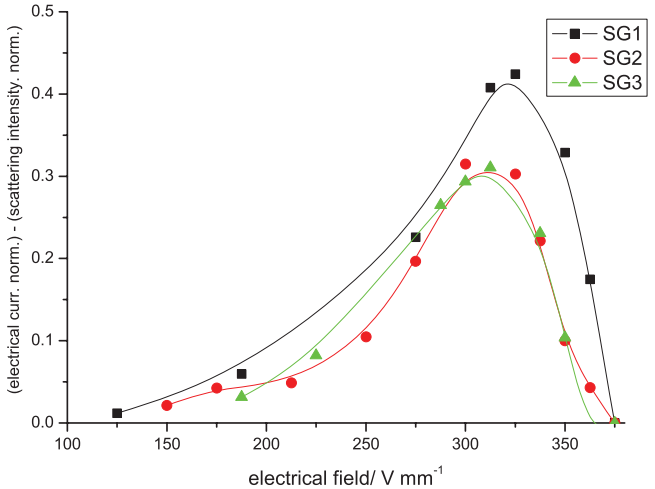

FIG. 3. Difference between normalized electrical current x EF and normalized scattered intensity x EF curves, from data of Fig. 2.

amount of water adsorbed, which, in turn, is related to surface properties such as area, porosity, and pore diameter.

B. Dehydration experiments in the electrical field

In these experiments, the idea was to slowly dehydrate the silica particles in constant dc electrical field (375 V mm^{-1}) and to monitor the behavior of charge transport by these particles when the hydration layer becomes thinner and the outer hydration layer is nearer to the surface. As can be observed in Fig. 4, the electrical current changes while the dehydration proceeds, suggesting that the thickness of the water layer adsorbed influences the transport of electrical charge by the particles.

It is important to point out that in a preliminary study using the same range of the experimental values of relative humidity inner of the cell (RH_{in}) and around of the cell (RH_{box}), the electrical current transported through the air was lower than 0.005 μA and considered negligible for the experimental results.

The curves in the Fig. 4 show the electrical current transported by each silica sample during the slow dehydration process under a constant dry airflow (1 L min^{-1}).

From these curve profiles, three important characteristics are noted,

- when the dehydration proceeds gradually, the electrical current initially decreases, reaching a minimum value, then increases to a maximum value and, finally falls to zero. The time that the minimum and maximum current values occur seems to be related to physical properties of each material. Figure 4(b) shows that the time of the i_{peak} with the dehydration is directly proportional to surface area and inversely proportional to the pore diameter.
- The three silica samples have similar maximum values of electrical current (*peak current*, i_{peak}) suggesting that along with dehydration, the "electron affinity" of the superficial water is, for some reason, modified. One hypothesis is that the electron affinity can be related to the space organization acquired by water due to the structural effect imposed by the silica surface, which decreases with distance from the surface.
- With constant surface humidity no significant changes were observed in the electrical current during the time of exposure in the electrical field (Fig. 4(a)) showing that the capacity of transport of charges by particles was maintained unaltered, without any degradation under the field of 375 V mm^{-1}, suggesting that a *Faradaic* process and, consequently, ion generation seems less probable.

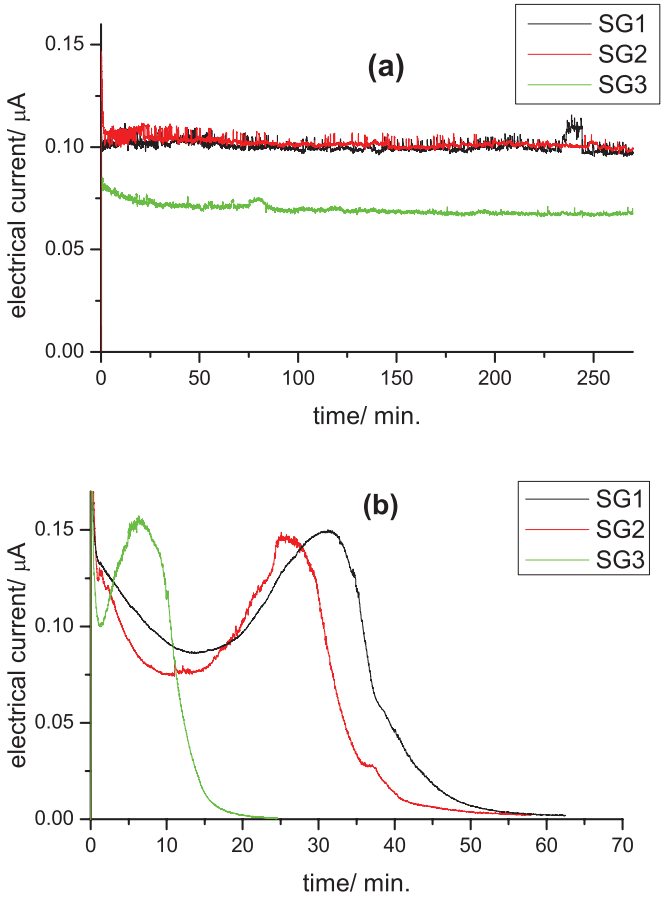

FIG. 4. Electrical current vs. time: (a) constant humidity and (b) slow dehydration of the hydrated silica by dry air flow (1 L min^{-1}), under constant electrical field (375 V mm^{-1}).

C. Kinetics of dehydration

Figure 5 shows the curves of electrical current and the kinetics of dehydration with dehydration time.

In Figs. 5(a) and 5(b), a common behavior in the gravimetric curves can be observed with three kinetic constants of dehydration due to the different interaction forces between the molecules of water and the silica surface. It is known that the interaction energy between water and the silica surface is higher near to the surface than away from the surface, where the structure of the "bulk water" prevails.

Figure 5(c) shows that the gravimetric curve of sample SG3 has only two kinetic constants. This can be attributed to the inexistence or a very small content of bulk water, so that the interval between the weighings and the precision of the balance impeded the detection of the last step of the gravimetric curve. The low frequency of the weight is a limitation imposed by the experimental procedure.

The correlation of electrical current and gravimetric curves show that the period of time of the second dehydration kinetics coincides with the maximum of the electrical current, reinforcing the hypothesis that the "electron affinity" is associated with the type of superficial water and, consequently, its spatial organization.[37,38]

D. Electrical current vs. RH_{in} and rate of variation of the number of particles in the flow during dehydration

To discard relationships between RH_{in} changes and the electrical current, the RH_{in} was monitored during the dehydration and the results are shown in Fig. 6.

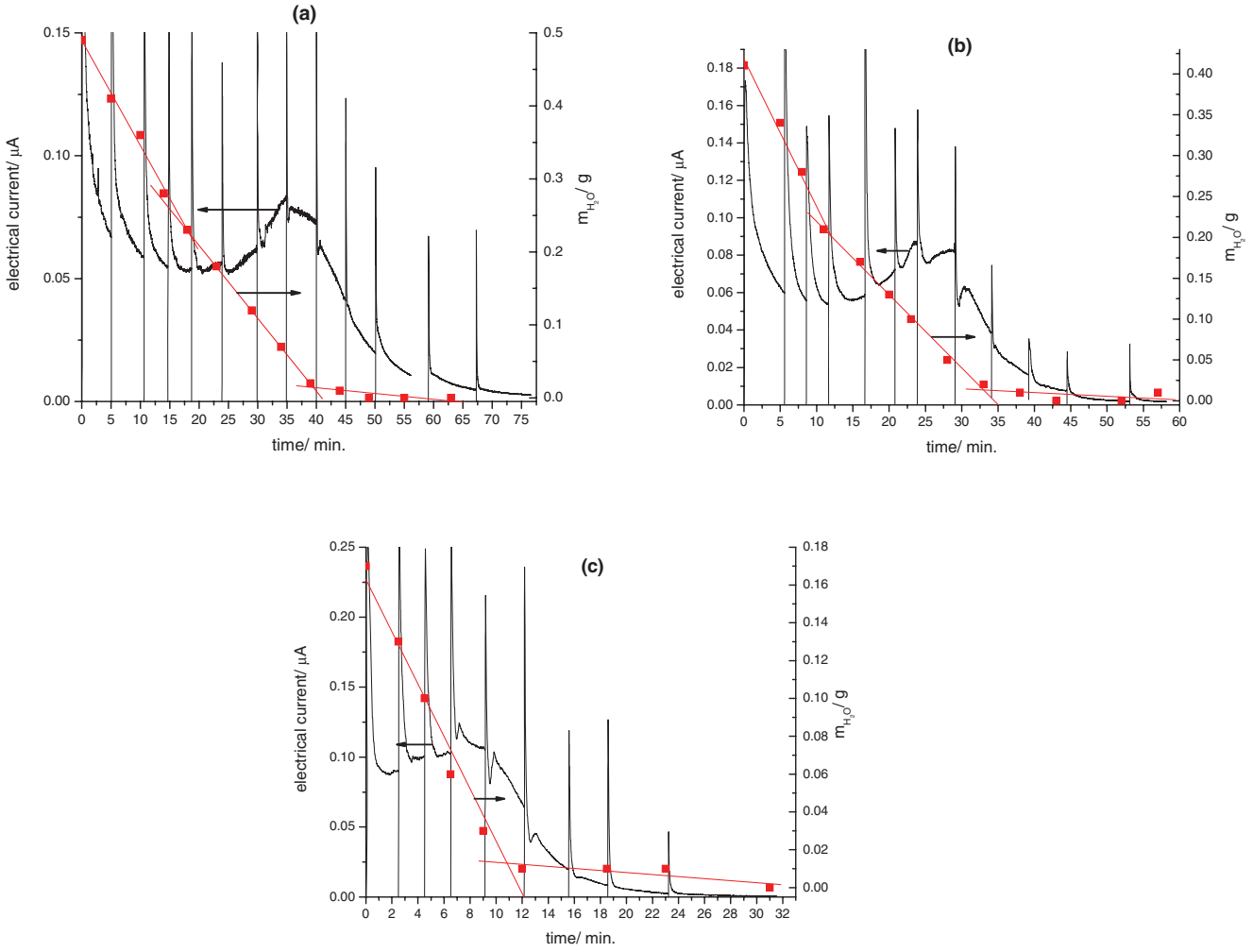

FIG. 5. Averaged curves and kinetics of dehydration of silica samples during dehydration with a flow of dry air (1 L min.$^{-1}$, 298 ± 1 K) under constant electrical field: (a) SG1; (b) SG2, and (c) SG3. The electrical current peaks correspond to the capacitive current, characteristic of the shifting of the electrodes after the weighing of the system (cell + silica).

Figure 6 indicates that the electrical current transported by the silica particles increases even when the RH_{in} decreases, giving maximum values between 30% and 45% of RH_{in}.

Although the data presented suggest that the electrical current is associated with organized water adsorbed on silica, it is possible that the increase of electrical current along with dehydration, up to the peak value (Figure 4(b)), occurs due to an increase in the number of particles flowing in the EF. To evaluate this hypothesis, the monitoring of variations in the number of particles flowing as functions of the EF was made by light-scattering. The response of the photodetector, in volts, is directly proportional to the intensity of light that arrives at the detector. The results are shown in Fig. 7.

Analysis of these plots indicates that the electrical current does not follow the same tendency of the rate of variation of the number of particles flowing since it was observed that, starting from t = 0 s, the electrical current declines while the number of particles flowing increases. After reaching a minimum, the electrical current increases until reaching a peak, while the number of flowing particles declines continually to the end of the dehydration, confirming the hypothesis of that the "electron affinity" of the adsorbed water changes along with gradual dehydration.

IV. MODEL OF FORCES

To try to explain the experimental observations, a model was developed to evaluate the significant forces that act on an ideal system composed of two spherical particles of silica gel in contact, as represented in Fig. 8. As the silicas used in this work have irregular shapes, the objective with this approach is to know the magnitude of each force component and to define those that are significantly acting on this particle.

For a silica particle to migrate vertically to the positive electrode, the electrostatic force ($\vec{F}_E$) should annul the opposite forces ($\vec{F}_{op}$) acting on this particle, which is composed of the capillary force ($\vec{F}_C$), van der Waals forces ($\vec{F}_{\mathrm{vdW}}$), the electrostatic forces ($\vec{F}_{elect}$), the binding forces ($\vec{F}_B$), and the gravitational force ($\vec{F}_g$), according to Eq. (1),[39]

$$\vec{F}_{op} = \vec{F}_C + \vec{F}_{\mathrm{vdW}} + \vec{F}_{elect} + \vec{F}_B + \vec{F}_g. \qquad (1)$$

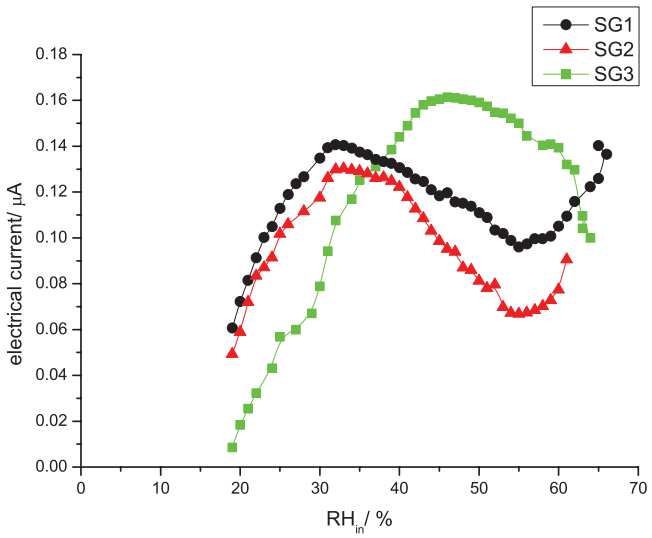

FIG. 6. Correlation curves between the relative humidity inside the cell and the current for silica samples. These experiments were started with the samples hydrated to equilibrium (RH = 74% and T = 298 K).

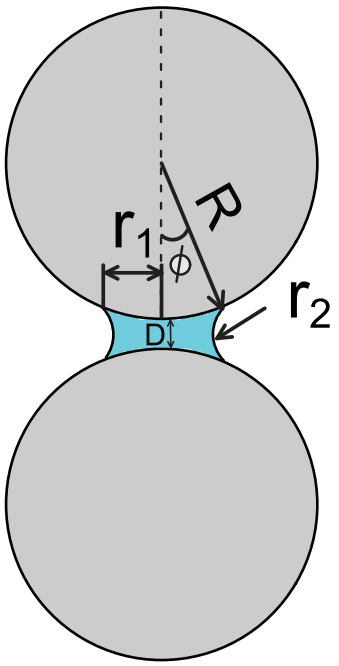

FIG. 8. Model used to estimate van der Waals and capillary forces. Conditions: $R = Xm/2$; $\phi \sim 0$; r2 $\gg$ r1; $D \ll R$.

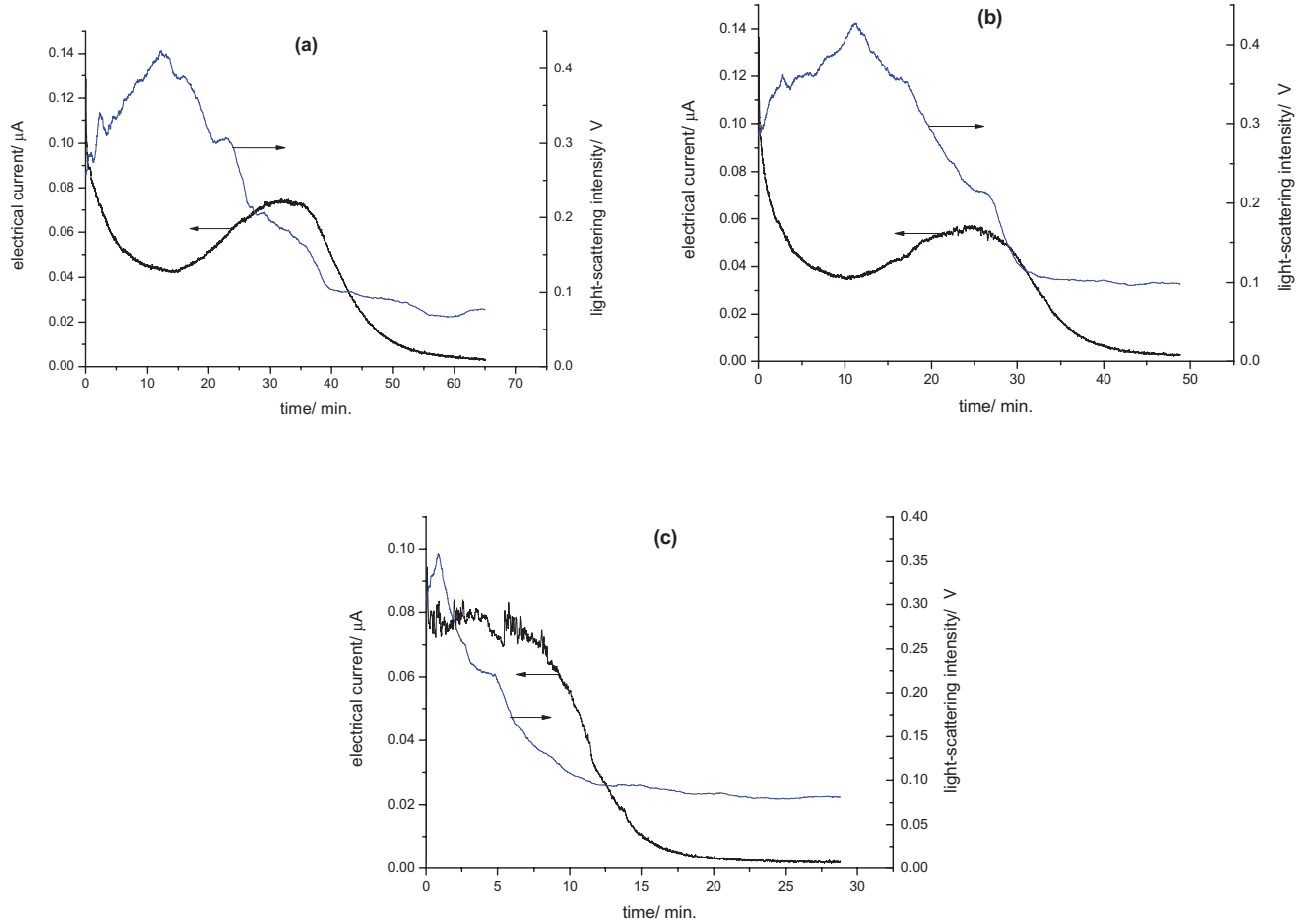

FIG. 7. Curves of light-scattering intensity and current as functions of the dehydration time, under constant electrical field and dry air flow (375 V mm^{-1} and 1 L min^{-1}): (a) SG1; (b) SG2, and (c) SG3.

As the silica gel surface has no unoccupied chemical bonds and it should not have electrical charges, so it is assumed that components $\vec{F}_B$ and $\vec{F}_{elect}$ can be neglected.[39]

The estimate of each component of $\vec{F}_{op}$ was made considering the mean size of the particle (X_m), from Table I, as the diameter of the spheres of silica used in an idealized model. The estimate of the magnitude of each force component is discussed separately below.

A. Gravitational force

The gravitational force ($\vec{F}_g$) is the simplest component of force and can be calculated by Eq. (2), where g = 9.8 m s^{-2}, d_B = bulk density[43] (Table I) and X_m = diameter of particle,

$$\vec{F}_g = \frac{\pi \vec{g} d_B X_m^3}{6}. \quad (2)$$

From Eq. (2), the $\vec{F}_g$ acting on a particle of silica gel is estimated to be between 12 and 16 μN for dry particles. For hydrated particles in equilibrium under the conditions described in Sec. II, this force is estimated to be between 14 and 25 μN.

B. van der Waals forces

The van der Waals *force* ($\vec{F}_{\text{vdW}}$) is proportional to the contact surface and the dielectric constant of the medium in which the particles are immersed. Therefore, this component of force must be estimated for two conditions: dry and hydrated silica particles. The model shown in Fig. 8 was used to calculate $\vec{F}_{\text{vdW}}$, using Eq. (3), where A = *Hamaker* parameter = 10.38×10^{-20} J for air, and 1.9×10^{-20} J for water, and D = 0.2×10^{-9} m for dry, and 2.0×10^{-9} m for hydrated silica with approximately three layers of water,[40]

$$\vec{F}_{\text{vdW}} = \frac{AR}{12D^2}. \quad (3)$$

For the conditions described, the value of $\vec{F}_{\text{vdW}}$ was estimated as 0.034 μN for hydrated particles connected by capillary bridges, as shown in Fig. 8. As can be seen, the $\vec{F}_{\text{vdW}}$ is considerably lower than $\vec{F}_g$ for particles hydrated at equilibrium in the chamber with 74% relative humidity (see Sec. II). However, the $\vec{F}_{\text{vdW}}$ between two dry particles is estimated as 18 μN.

C. Capillary force

The last component of $\vec{F}_{op}$ is the capillary force ($\vec{F}_c$) which, for macroscopic particles, is described by Eq. (4), where $R = X_{m/2}$, γ = water surface tension = 72.14 mN m^{-1} (298 K), and θ = contact angle = ~0° for a water/silica interface,[39,40]

$$F_C = 4\pi \gamma_L R \cos\theta. \quad (4)$$

The $\vec{F}_c$ estimated by Eq. (4) is found to be 77 μN. As shown by this equation, for macroscopic particles, $\vec{F}_c$ is independent of the hydration. This approximation is correct for smooth surfaces. For microrough surfaces, the $\vec{F}_c$ increases with the surface humidity and can be two times the estimate made by Eq. (4) (Refs. 40 and 41).

D. Conclusions about opposite force ($\vec{F}_{op}$)

With the estimated values of $\vec{F}_{op}$ components acting on a silica particle, it was possible to consider that only $\vec{F}_g$ and $\vec{F}_c$ components are significant. The intensity of both forces increase with hydration. During dehydration, $\vec{F}_c$ goes to zero and $\vec{F}_{op}$ becomes equal to $\vec{F}_g$, as shown by Eqs. (1)–(4). According to these estimates, $\vec{F}_c + \vec{F}_g$ corresponds to ~90 μN. $\vec{F}_{\text{vdW}}$ is negligible for hydrated particles (only 0.034 μN for three water layers) but it increases to 18 μN when the particles are completely dried. These forces will be used to analyze qualitatively the electrostatic phenomenon observed.

E. Steps of the process of charge transport

To discuss the experimental observations, electrical charge transport was separated into *three elementary steps*, where each one can directly influence the process of charge transport and, consequently, the experimental results.

In the following treatment, the water film on the silica surface will be considered as a *pseudocrystal* having an electronic structure of bands, similar to insulating bands, in such a way that the electrons are injected from the electrode directly into the conduction band of this film and the electron is in a *quasifree* state.

In the *first step*, it is considered that the surface water film on one particle merges with that on particles with which it is in direct contact, forming a continuous film covering all particles. When the applied potential between the electrodes is increased at some moment, the energy of the electrons (*Fermi level, E_f*) of the grounded electrode becomes higher than the energy of the conduction band (CB) of the water film adsorbed on the silica, and the electrons of this electrode are spontaneously transferred to this band and this water film acts like a continuous electrical conductor covering all particles, distributing the electrical charge injected by the grounded electrode over the surface of all interconnected particles. When the electrical charge on one particle reaches a value in which the electrostatic force ($\vec{F}_E$) acting on the particle annuls $\vec{F}_{op}$ (Eq. (5)), the connection with the other particles due to surface film is broken and the particle is hurled to the positive electrode,

$$\vec{F}_{op} = \vec{F}_E. \quad (5)$$

The *second step* is the migration and comprises the process between the moment in which the particle starts moving and that in which this particle collides with the positive electrode. The speed of migration depends on the acceleration at the moment in which the particle breaks away. Since component $\vec{F}_c$ is eliminated when the capillary bridges are broken, the particle will be transported with acceleration proportional to $\vec{F}_c$, according to Eq. (6), where q_{EC} and $\vec{F}_{\text{EC}}$ are the electrical charge and the electrostatic force necessary to annul the capillary force and $\vec{E}$ is the intensity of electrical

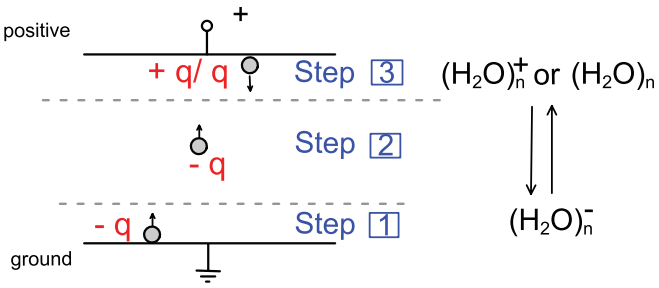

FIG. 9. Schematic representation of the three steps suggested for the charge transport process with hydrated sílicas.

field,

$$\vec{a} = \frac{\vec{F}_{EC}}{m} = \frac{q_{EC}\vec{E}}{m}. \quad (6)$$

The *third step* (final step) comprises the moment in which the hydrated particle collides with the positive electrode and, during contact, transfers all the excess of charge added into the CB of the water film and, if possible, also part of the electrons of the valence band (VB). The electrons in the VB of the water can be removed when the Fermi level (E_f) of the electrode becomes smaller than the VB of the water film.

A graphical representation of this "three step mechanism" is shown in Fig. 9.

The following discussion will be based on this model of forces and the ideal description of the charge transfer process.

V. DISCUSSION

Recent papers have shown that water can be a more important component in the electrification of surfaces than simply to increase conductivity and to facilitate the dissipation of electrical charges[24]. It was shown that water in the condensed state can store ionic[24] or electronic[25] charges.

In this work, the function of a thin film of water on a silica surface in the electrification process of these particles was investigated. For this, the hydrated silica particles were electrically charged on the grounded electrode in an electrical field of up to 375 V mm^{-1} (voltage of 30 kV). Patterns of charge transport as a function of the superficial humidity for three silica samples were observed that had similar chemical characteristics but different superficial (physical) properties.

To explore this phenomenon, the charge transported by hydrated silica in an electrical field was studied under two different conditions: (a) the surface humidity was maintained unchanged and the electrical field was scanned between 0 and 375 V mm^{-1}; (b) the electrical field was maintained constant at 375 V mm^{-1} and the surface humidity was decreased by a flow of 1 L min^{-1} of dry air. These two conditions are discussed separately in the following paragraphs.

A. Experiments with constant surface humidity

In the first experimental condition the charge transport by hydrated silica was studied maintaining constant the mass of water adsorbed on silica particles (water adsorbed up to equilibrium at 74% relative humidity) and the electrical field intensity was scanned between 0 and 375 V mm^{-1}. Under this experimental condition, the curves of electrical current vs. electrical field intensity (Figs. 2(a) and 2(b)) show that all samples behave in the same way as functions of the electrical field intensity, which is more evident in the normalized curves shown in Figs. 2(c) and 2(d). A peculiar characteristic of these curves is the sudden increase in the rate of electrical charge transported at 225 V mm^{-1}, which can occur by an increase in the number of particles flowing in the electrical field or by an increase in the number of electrical charges transported by each particle.

Comparing Fig. 2(a) with the Fig. 2(b), it is observed that the rate of charge transport increases more rapidly than the number of particles flowing up to ~310 V mm^{-1}. This can be better observed by the difference between these two curves, as shown in Fig. 3. Therefore, the first hypothesis can be neglected and it is possible to attribute the increase of the rate of charge transport, to the number of charges transported by the particle.

According to the treatment shown in Sec. IV, by analyzing the forces acting on a particle with constant mass exposed to an electrical field, it is possible to conclude that the number of charges injected by the grounded electrode into the electronic structure of the water layer, generating hydrated electrons $(H_2O)_n^-$, depends on the opposite force ($\vec{F}_{op}$) because when $\vec{F}_E$ annuls $\vec{F}_{op}$ the surface film is broken and the particle is hurled to the positive electrode, the electrical charging is suddenly interrupted. As the hydration and, consequently, the total mass (silica + water) are constant, the $\vec{F}_{op}$ ($\vec{F}_c$ + $\vec{F}_g$) can be considered constant and the number of electrical charges that satisfies Eq. (5) should be constant. This does not justify the experimental observations. The van der Waals *force* ($\vec{F}_{vdW}$) is negligible in these experimental conditions.

Based on the *third step* of charge transport process, when a hurled particle collides with the positive electrode, the electrical charges are transferred to this electrode. If only the excess of electrons added in the CB of the water layer is removed, the rate of charge transfer would be constant. But, if during the short time contact with the positive electrode not only the excess of injected charges is transferred from the CB of the water film to the electrode but also part of the electrons in the VB, making the particle positively charged after contact, more charges would be transported by each particle and the break observed at ~225 V mm^{-1} in the curves shown in Figs. 2(a) and 2(c), could be related to the beginning of the transfer of electrons from the VB, when the E_f (energy of outermost electrons) of the electrode falls below of the top of the VB of water film. With this suggestion, this break in the curves of Figs. 2(a) and 2(c) can be a manifestation of *band gap* and the electrical field in which it occurs can be evidence of the energy of the *band gap* of the water film structure.

Experiments with both superficial humidity and electrical field constant have shown that the electrical current transported by the particles is constant with time (Fig. 4(a)), suggesting that the electrical charge on the particles is mainly from electrons injected by the grounded electrode into the adsorbed water film on the silica particles. In a *Faradaic* process

the chemical species are consumed and the electrical current must decrease with time in electrical field.

B. Experiments with electrical field constant

To explore the effect of the thickness of the water film on charge transport, the silica gel was slowly dehydrated by a constant flow of dry air through the cell, reducing the thickness of the water film adsorbed on the silica surface.

In the curves of electrical current versus dehydration time, shown in Fig. 4(b), the rate of charge transport shows a characteristic behavior with dehydration, increasing to a maximum value (i_{peak}) and decreasing up to the end of dehydration. Based on these experimental observations, in the proposed model it can be supposed that the rate of transport of charges is influenced by variations of number of particles flowing between the electrodes and the variation of the humidity in the cell (RH_{in}). However, by monitoring the variations of the number of particles flowing by light-scattering, it was observed (Fig. 7) that the number of particles does not vary proportionately to the rate of charge transport. This experimental data allow discarding the effect of increases in the number of flowing particles between the two electrodes in the profile of the curves shown in Fig. 4(b). Similarly, a possible increase in the relative humidity in the cell (RH_{in}), increasing the electrical conductivity of the air, cannot explain the profile observed in the curves in Fig. 4(b) because, as can be seen in Fig. 6, the (RH_{in}) decreases continuously throughout the experiment time.

After discarding RH_{in} and the number of particles flowing as responsible for the profile of the curves shown in Fig. 4(b), a model of forces (Sec. IV) was applied to try to explain the charge transport under these experimental conditions. According to Eq. (5), and as discussed for the curves in Fig. 3, the transport of electrical charges at the *first step* is limited by $\vec{F}_{op}$, composed mainly of $\vec{F}_g$ and $\vec{F}_c$, which decrease with dehydration. It is important to comment that $\vec{F}_{vdW}$ is initially negligible ($\sim$0.034 μN with $\sim$3 water layers) and increases with dehydration up to 18 μN for completely dried particles. Thus, $\vec{F}_{op}$, considering the $\vec{F}_{vdW}$ component, would decrease from $\sim$90 μN to $\sim$30 μN. However, considering this force component in $\vec{F}_{op}$ does not modify the qualitative analysis of the proposed model.

In the *second step*, migration, the acceleration in which the silica particle is hurled is proportional to F_{EC}, which also decreases along with dehydration. Thus, the increase of rate of the charge transport with dehydration until i_{peak} (Fig. 4(b)) can be attributed, mainly, to the *third step* of the suggested model of charge transport, in which the charge transfer depends on the energy of the electronic bands of water and the E_f of the positive metallic electrode. The increase in the charge transport can be explained because, in addition the electrons added into the *CB,* part of electrons of the VB of water are removed during contact with this electrode. However, for the positive electrode at constant potential (30 kV; 375 V mm^{-1}) to remove more charges from the VB of the water along with dehydration, the energy of this band must be modified because the energy of the electrons of the metallic electrode (E_f) is constant with temperature and with applied potential constants.

This hypothesis is based on studies that show that, in dielectric relaxation experiments, the molecules in the first adsorption layer are strongly bound to the surface, changing the geometries and, consequently, the energy of the hydrogen bond between water molecules.[18,19,21,42] Therefore, it can be suggested that, with the decreasing thickness of the hydration layer, through dehydration with a dry airflow, the more external layers become closer to the surface, the hydrogen bond energy decreases due to the influence of the surface silanol groups and the top of the VB of water increases, allowing part of the electrons in this band also to be transferred to the positive electrode, which could explain the increase in the electrical current during dehydration, as observed in the profile of the curves in Fig. 4(b). In Fig. 5, it can be observed that the increase of charge transport occurs when the water film reach a thickness of $\sim$1.5 statistical water layers and reaches the maximum value when there are $\sim$0.4 statistical water layers, corroborating this proposed model.

If this qualitative model is confirmed, it can become a good method to study the effect of the surface on the spatial organization of water. Theoretical papers have already predicted an increase of electronic affinity with the size of the water cluster and also with the alteration of angles and bond forces of isolated water molecules.[18,19,21]

VI. CONCLUSIONS

In this work, the electrical charges transported by hydrated silica particles and the role of surface water on this electrification phenomenon was investigated. The electrification phenomenon is much studied, however little understood. From the data presented, we have shown the participation of water in the observed phenomenon and its electrical behavior under an electrical field.

To assay the phenomenon, the charge transport process was separated into three elementary steps, of which the *first* and *third steps* depend on the relationship the between electronic bands of the water film and the *Fermi level* of the electrode, while the *second step* depends on the vertical migration between the two electrodes. Based on an idealized model, the forces acting on a silica particle were estimated and suggested some hypothesis to explain the observed results.

With this first analysis of this phenomenon, the charge transport process realized by hydrated silica seems to occur by electrostatic charging of the water film adsorbed on the silica, by injection of electrons into "conduction band" of this condensed water, which is directly dependent on the thickness of the water layer.

The possible alteration of the electronic properties of the condensed water on the surface shows the structural differences between the first and the other layers of adsorbed water, providing alterations in the electron affinity of the water condensed on the silica particles.

This paper presents a first qualitative analysis of this new phenomenon and much work is still needed to prove the mechanism shown here and to lead to a better understanding of this electrostatic phenomenon.

ACKNOWLEDGMENTS

The authors thank CNPq – Conselho Nacional de Desenvolvimento Científico e Tecnológico, Brasil, for financial support and Professor Carol H. Collins for critical review.

[1] F. Rouquerol, J. Rouquerol, and K. S. W. Sing, *Adsorption by Powders and Porous Solids: Principles, Methodology and Applications* (Academic, London, 1999).
[2] G. M. S. El Shafei, *Adsorption on Silica Surfaces*, Surfactant Science Series Vol. 90, edited by E. Papirer (Marcel Dekker, New York, 2000), p. 40.
[3] Q. Du, E. Freysz, and Y. R. Shen, Phys. Rev. Lett. **72**, 238 (1994).
[4] A. Bogdan, *Adsorption on Silica Surfaces*, Surfactant Science Series Vol. 90, edited by E. Papirer (Marcel Dekker, New York, 2000), p. 689.
[5] J. D. F. Ramsay and C. Poinsignon, Langmuir **3**, 320 (1987).
[6] P. G. Hall, A. Pidduck, and C. J. Wright, J. Colloid Interface Sci. **79**, 339 (1981).
[7] T. Takei and M. Chikazawa, J. Colloid Interface Sci. **208**, 570 (1998).
[8] K. Klier, J. H. Shen, and A. C. Zettlemo, J. Phys. Chem. **77**, 1458 (1973).
[9] P. Hall, R. T. Williams, and R. C. T. Slade, J. Chem. Soc., Faraday Trans. 1 **81**, 847 (1985).
[10] R. P. W Scott and S. Traiman, J. Chromatogr. **196**, 193 (1980).
[11] P. Staszczuk, M. Jaroniec, and R. K. Gilpin, Thermochim. Acta **287**, 225 (1996).
[12] H. Yamauchi and S. Kondo, Colloid Polym. Sci. **266**, 855 (1988).
[13] J. Yang, S. Meng, L. F. Xu, and E. G. Wang, Phys. Rev. Lett. **92**, 146102 (2004).
[14] P. C. Couto, B. J. C. Cabral, and S. Canuto, Chem. Phys. Lett. **429**, 129 (2006).
[15] G. Ohrwall, R. F. Fink, M. Tchaplyguine, L. Ojamae, M. Lundwall, R. R. T. Marinho, A. N. de Brito, S. L. Sorensen, M. Gisselbrecht, R. Feifel, T. Rander, A. Lindblad, J. Schulz, L. J. Saethre, N. Martensson, S. Svensson, and O. Bjorneholm, J. Chem. Phys. **123**, 054310 (2005).
[16] S. Hirofumi and H. Fumio, J. Chem. Phys. **111**, 8545 (1999).
[17] F. Willians, S. P. Varma, and S. Hillenius, J. Chem. Phys. **64**, 1549 (1976).
[18] D. M. Chipman, J. Phys. Chem. **82**, 1080 (1978).
[19] D. M. Chipman, J. Phys. Chem. **83**, 1657 (1979).
[20] H. M. Lee, S. B. Suh, P. Tarakeshwar, and K. S. Kim, J. Chem. Phys. **122**, 044309 (2005).
[21] P. C. Couto, S. G. Estácio, and B. J. Cabral, J. Chem. Phys. **123**, 054510 (2005).
[22] L. S. McCarty, A. Winkleman, and G. M. Whitesides, J. Am. Chem. Soc. **129**, 4075 (2007).
[23] G. P. Shpenkov, *Friction Surface Phenomena*, Tribology Series Vol. 29 (Elsevier, Amsterdam, 1995).
[24] R. F. Gouveia and F. Galembeck, J. Am. Chem. Soc. **131**, 11381 (2009).
[25] K. Ovchinnikova and G. H. Pollack, Langmuir **25**, 542 (2009).
[26] L. C. Soares, S. Bertazzo, T. A. L. Burgo, V. Baldin, and F. Galembeck, J. Braz. Chem. Soc. **19**, 277 (2008).
[27] D. H. Paik, I. Lee, D. Yang, J. S. Baskin, and A. H. Zewail, Science **306**, 672 (2004).
[28] A. Taylor, C. F. Matta, R. J. Boyd, J. Chem. Theory Comput. **3**, 1054 (2007).
[29] N. I. Hammer, J. Shin, J. M. Headrick, E. G. Diken, J. R. Roscioli, G. H. Weddle, and M. A. Johnson, Science **306**, 1154 (2004).
[30] K. Onda, B. Li, J. Zhao, K. D. Jordan, J. Yang, and H. Petek, Science **308**, 1154 (2005).
[31] A. E. Bragg, J. R. R. Verlet, A. Kammrath, O. Cheshnovsky, and D. M. Neumark, Science **306**, 669 (2004).
[32] C. E. Perles and P. L. O. Volpe, J. Chem. Phys. **133**, 241101 (2010).
[33] See http://www.datasheetcatalog.org/datasheet/BurrBrown/mXqyxtx.pdf (accessed on 01/03/2011).
[34] A. Root Ek, M. Peussa, and L. Niinisto, Thermochim. Acta **379**, 201 (2001).
[35] See http://www.discoverysciences.com/uploadedFiles/Home/MEDIA_Davisil.pdf (accessed on 30/03/2011).
[36] *Handbook of Chemistry and Physics*, edited by D. R. Lide, 85th ed. (CRC Press, New York, 2004–2005), Chap. 15, p. 37.
[37] V. V. Turov and I. F. Mironyuk, Colloids Surf., A **134**, 257 (1998).
[38] D. B. Asay and S. H. Kim, J. Phys. Chem. B **109**, 16760 (2005).
[39] X. Xiao and L. Qian, Langmuir **16**, 8153 (2000).
[40] J. Israelachvili, *Intermolecular and Surface Forces* (Academic, New York, 1985), p. 122.
[41] R. Jones, H. M. Pollock, J. A. S. Cleaver, and C. S. Hodges, Langmuir **18**, 8045 (2002).
[42] A. Bernas, C. Ferradini, and J. Jay-Gerin, Chem. Phys. **222**, 151 (1997).
[43] Bulk density is the density calculated with the apparent volume of a porous particle considering the pore void volume.